Letters in Applied NanoBioScience
Open-Access Journal (ISSN: 2284-6808)

Review
Volume 12, Issue 4, 2023, 140
https://doi.org/10.33263/LIANBS124.140

A Comprehensive Review on the Antimicrobial and Photocatalytic Properties of Green Synthesized Silver Nanoparticles

Srinatha Narayanaswamy [1,*], Rakesh Bhaskar [2], Rudresh Kumar Kondapura Jayadevappa [3], Suresh Kumar Madathil Ramachandran [1], Madhu, Ananda Prasad [4]

1 Department of Physics, RV Institute of Technology and Management, Bengaluru, 560 076 India; srinatha007@gmail.com (S.N.);
2 Department of Life Sciences, Christ (Deemed to be University), Hosur Road, Bengaluru, 560 029 India
3 Department of Chemistry, RV Institute of Technology and Management, Bengaluru, 560 076 India
4 Department of Physics, Dayananda Sagar College of Engineering, Kumaraswamy Layout, Bangalore 560 078, Karnataka, India

Scopus Author ID 56308062400
Received: 11.01.2022; Accepted: 5.02.2022; Published: 8.10.2022

Abstract: With the advancement of technology, there is a growing demand for new nanoparticles that are viable, eco-friendly, non-toxic, and non-hazardous, as well as having unique chemical and physical properties. Silver nanoparticles are currently promising for antibacterial, antimicrobial, and photocatalytic applications. Because of their toxicity, nanosilver particles are now widely used in various applications, including cosmetics, clothing, sunscreen, medicinal, sensing, antibacterial, antimicrobial, and photocatalytic. The importance of plant extracts in the synthesis of AgNPs is emphasized. The various mechanisms and characterization techniques used in the study of silver nanoparticles will also be covered. This review also discusses the role of green synthesized AgNPs in antimicrobial and photocatalytic applications, which adds to our understanding of improving health, and the environment and preventing contagious diseases.

Keywords: green synthesis; silver nanoparticles; antibacterial; antimicrobial; photocatalysis.

1. Introduction

The potential interest in nanoparticle research and its applications in the fields of therapeutics, environmental science, and material science has opened a new window in the scientific community for determining the safest methods of nanomaterial synthesis, utilization, and disposal, as well as removing any potential harmful effects on nature [1-3]. Ayurvedic Bhasma is an example of ecologically friendly nanoparticles from the past [4]. Ayurvedic Bhasma is believed to be highly safe and cost-effective when compared to contemporary metal-based nanomedicines [5-7]. For decades, physical and chemical nanoparticle synthesis methods have been utilized to generate homogeneous, monodispersed, spherical metal nanoparticles [8-9]. However, because it is simple, fast, environmentally friendly, and cost-effective, transforming bulk materials into nanomaterials utilizing microorganisms and plant material has emerged as a viable alternative to standard physical and chemical procedures in recent years [10-11]. Because of their high catalytic, electrical, magnetic, and antimicrobial activity, nanoparticles with a high specific surface area to volume ratio have gained popularity in the

field of research and application, and they could be used in sensors, catalysts, surface-enhanced Raman spectroscopy, and biomedicine [12–17].

Silver nanoparticles (AgNPs) are crucial in the current scenario due to their different optical, thermal, electrical, and biological characteristics[12–17], hence finding many applications in the present technology, depicted in Figure 1. Many reports of physical, chemical, and bio-mediated synthesis techniques [18–20]. Chemical reduction, electrochemical, and photochemical reduction are the most commonly used chemical techniques [20]. Evaporation-condensation and laser ablation are two additional important physical techniques [21-22]. On the other hand, chemical reduction with organic and inorganic reducing agents is the most common approach for generating AgNPs [20]. To date, several reducing agents have been used to reduce silver ions (Ag+) in aqueous and non-aqueous solutions, including sodium citrate, sodium borohydride (NaBH4), ascorbate, N-dimethylformamide (DMF), elemental hydrogen, polyol process, N, and poly (ethylene glycol)-block copolymers and Tollens reagent, [18–20]. In producing nanoparticles, microorganisms such as bacteria, fungi, protozoans, and other microbes are utilized [23–25]. Extracellular synthesis is more advantageous than intracellular synthesis because nanoparticle separation is much easier in the former. Furthermore, anaerobic microorganisms like Treponema species, Clostridium, Microbes, and enzymes act as reducing agents, and various microorganisms like fungal mycelium, bacterial strains of *E. coli*, *Staphylococcus*, *Salmonella* species, and others have been studied and found to be well-known reducing agents [18, 19, 23-25]. Among all methods, biosynthesized nanosilver nanoparticles are suitable for a wide range of applications, including pollution abatement, pharmaceutical applications, and so on, due to their remarkable properties such as antibacterial, chemical stability, and rigorous catalytic activities [17-25].

On the other hand, there is a growing demand for ecologically friendly procedures that avoid using toxic and hazardous chemicals in their synthesis, a process known as Green synthesis [15, 18-19]. Green synthesis techniques have acquired considerable lead in environmental conservation, and efforts to eradicate hazardous wastes and biosynthesized nanoparticles are gaining popularity due to their non-toxicity, environmental safety, and non-hazardous properties. The green synthesis technique has been shown to be a straightforward and ecologically friendly method for producing silver nanoparticles using plant extract [18-19]. This technique has an advantage over physical and chemical methods due to its non-toxic and non-hazardous nature and the improved conditions for synthesizing metal nanoparticles. Green synthesis offers the additional benefits of being economical, having a simple single-step method, being readily scaled up for large-scale synthesis, and not needing high pressure, energy, temperature, or hazardous chemicals [18-19,25]. The extract derived from various sections of plants, such as leaves, fruit, flower, bud, pod extracts, and so on, is used as a reducing agent in the green synthesis process to reduce metal ions to metal nanoparticles. Phytochemicals present in plants and their different sections play an essential role in creating nanoparticles. Terpenoids, flavones, ketones, aldehydes, amides, amino acids, and carboxylic acids are important active components in the production of nanoparticles [18, 25]. Plant extracts such as aloe vera [26], pineapple [27], Arecaceae [28], ficus [29], neem [30], Nyctanthes [31], Morus [32], Hydrilla [33], *Phyllanthus amaru*s [34], *Rosa Indica* [35], and others have been utilized in green synthesis, as described in the literature. Green synthesized silver nanoparticles were used in a variety of applications, including antimicrobial [18-19, 25],

photocatalytic/dye degradation [36], biosensors [37], wastewater treatment [38-39], tissue engineering [40], cosmetics [41-42], coatings [43-44], drug delivery systems [45], and so on.

This review study illustrates the present state of the art and techniques for green synthesis of silver nanoparticles utilizing various plant extracts and their prospective uses. We also discuss the potential mechanisms for silver nanoparticle reduction and the procedures for various characterization techniques used to characterize silver nanoparticles for their potential properties in various applications, such as antibacterial, antimicrobial, and photocatalytic dye degradation.

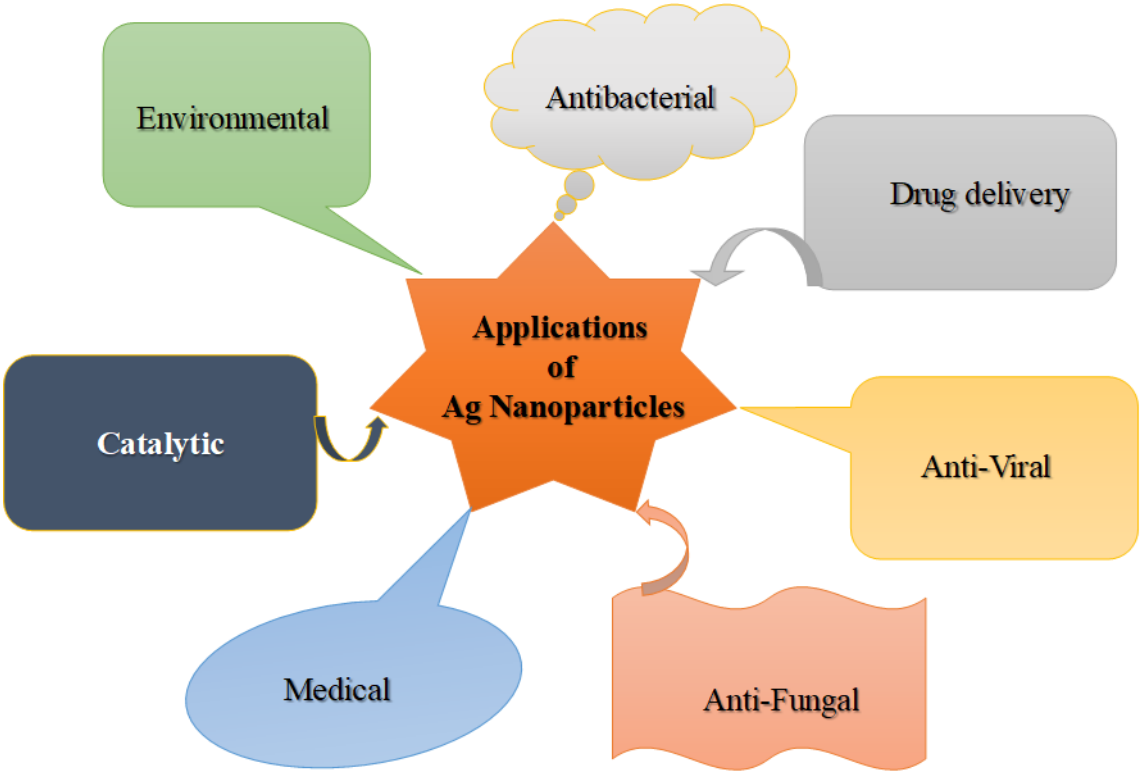

Figure 1. Potential applications of green synthesized silver nanoparticles.

2. Synthesis of Silver Nanoparticles

The green approach is utilized to synthesize silver nanoparticles using the following general technique. Figure 2 depicts a schematic illustration of the green synthesis method for producing silver nanoparticles. To begin, a sufficient amount of silver nitrate ($AgNO_3$) (10 mg) is dissolved in de-ionized water (50 ml) to fill the beaker. The beaker is coated with aluminum foil to prevent silver photodegradation. Simultaneously, a tiny amount of plant extract (5 mL) is dissolved to obtain the necessary concentration in de-ionized water (50 mL). The prepared plant extract will be added drop by drop to the silver nitrate solution and continually agitated at room temperature until the solution turns golden brown. The development of color demonstrates the reduction and synthesis of silver nanoparticles (golden brown). Different factors, such as synthesis temperature, pH, and synthesis duration, among others, may be used to regulate the size of the silver nanoparticles and the pace of synthesis. The mechanism of silver nanoparticle generation is as follows:

$$AgNO_3 + H_2O\ (DI) \longrightarrow Ag^+_{(aq)} + NO_3^-{}_{(aq)}$$

$$Ag^+_{(aq)} + NO_3^-{}_{(aq)} + \text{Plant Extract (water)} \xrightarrow{e^-} Ag^0\ (NPs)_{(aq)} + \ NO_2^- \ ()$$

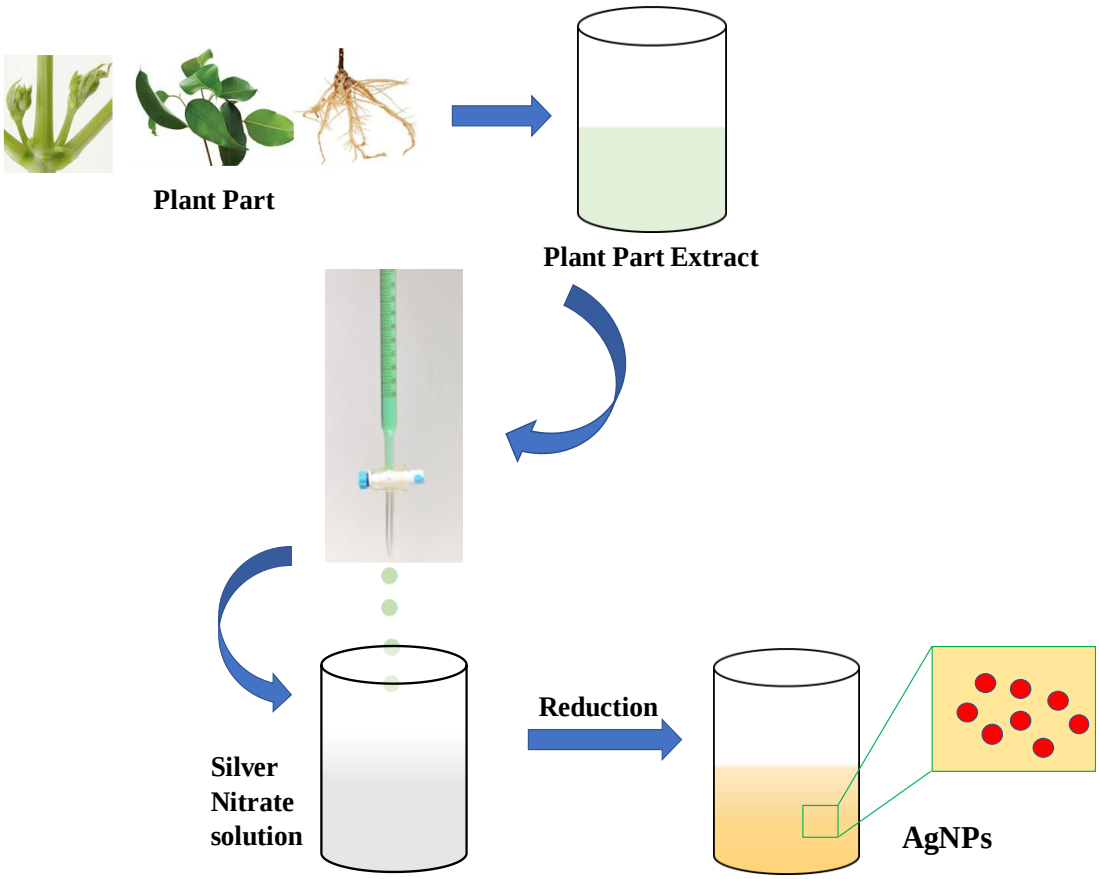

Figure 2. Schematic representation of the green synthesis of silver nanoparticles.

3. Characterization/Measurement Techniques

3.1. UV-Visible spectroscopy (UV-Vis).

In addition to the color change throughout the synthesis, UV-Visible spectroscopy can validate the production of silver nanoparticles. Generally, the absorbance spectra of the produced silver nanoparticles (in aqueous) will be recorded in the wavelength range of 300 nm to 800 nm. The distinctive peak of spherical silver nanoparticles, surface plasmon resonance (SPR), can be observed in the recorded absorbance spectra of about 420 nm. The concentration of silver nanoparticles in the solution is indicated by the strength of the SPR peak.

3.2. X-ray diffraction (XRD).

It is worth noting that the silver nanoparticles are produced in an aqueous media. To conduct XRD investigations, powder or film form is necessary. As a result, the produced samples (aqueous solution) may be centrifuged to get the concentration of silver nanoparticles, or the solution may be dried onto a glass plate to form a sufficiently thick film containing silver nanoparticles. The crystallinity of the slides will next be determined using an X-ray diffractometer. The acquired XRD patterns of silver nanoparticles will be compared to the conventional JCPDS pattern for phase purity and structural alterations. Furthermore, Scherer's method [46] will be used to calculate the crystallite size (the size of the silver nanoparticles).

$$D = \frac{k\lambda}{\beta cos\theta}$$

where, k is the Scherer's constant, λ is the wavelength of the x-ray used, β is the full with half maximum, and θ is the Bragg angle.

3.3. Scanning Electron Microscopy-Energy Dispersive X-ray Spectroscopy (SEM-EDS).

A Scanning Electron Microscope (SEM) is an imaging instrument used to investigate the surface morphology of materials at magnifications of up to 100,000X. A scanning electron microscope gets its name from the fact that pictures are acquired by scanning the surface of a sample with an electron beam and detecting the electrons scattered from the surface of the sample. An electrically conducting sample, such as a metallic sample, may often be examined without significant sample preparation. On the other hand, electrically insulating materials, such as polymers, biological samples, ceramics, and glasses, may require a small coating of electrically conductive material, such as gold or carbon, to produce better pictures. The morphology, such as voids, fractures, porosity, agglomeration, grain distribution, and average grain size, was assessed by SEM microscopy. For thin films, on the other hand, the cross-sectional SEM aids in estimating the thickness of the film on the substrate adhesively, and layered structure, if any, may be investigated. The X-rays produced by electrons scanning the material's surface can be examined using an Energy Dispersive X-ray Spectrometer (EDS) attachment. The quantitative information on the chemical composition of the sample's contents can also be calculated. In other words, EDS is best suited for identifying and mapping the elements present on a sample's surface.

3.4. High-Resolution Transmission Electron Microscope (HR-TEM).

The transmission electron microscope (TEM) is well-known for being a highly effective, efficient, and flexible imaging instrument in material research. Transmission electron microscopy (TEM) pictures with high resolution (HR-TEM) show structures at the atomic scale. HRTEM is the most effective approach for determining the size and dispersion of nanoparticle samples. HRTEM also aids in precisely estimating the structure, distribution, and size of particles with great resolution. HR-TEM allows a more accurate examination of the sample's morphology. The HRTEM picture may also be subjected to Inverse Fast Fourier Transformation (IFFT) to estimate the d-spacing of the crystalline sample, allowing the orientation of the crystallites to be calculated. It aids in estimating the presence of contaminants that the XRD could not identify owing to its limits. On the other hand, Selected Area Electron Diffraction (SAED) is a valuable method for identifying crystal structure and structural parameters such as d-spacing and lattice parameters. SAED patterns are composed of diffracted ring patterns, with each ring corresponding to a satisfied diffraction state of the sample's crystal structure. For this d, – spacing values and related (h k l) values may be calculated using conventional JCPDS patterns [46].

3.5. Fourier Transform Infra-Red Spectroscopy (FTIR).

In green synthesis, FTIR spectra aid in identifying the potential molecules responsible for reducing silver (Ag+) ions into metal silver (Ag) nanoparticles. The FTIR spectroscopy method will be used to record the absorbance/transmittance spectra. The existence of peaks/bands in the acquired spectrum shows the presence of distinct species' molecular vibrations in the processed samples.

3.6. Antibacterial.

The antibacterial activity of silver nanoparticles may be studied using (a) the broth dilution method and (b) the agar well diffusion method.

In the broth dilution method, a known volume of sterilized liquid medium (broth) is placed in test tubes (Figure 3). A known volume of pure bacterial culture is evenly distributed throughout the tubes. Multiple volumes/concentrations of the nanoparticle solution are added to determine the lowest concentration that suppresses bacterial growth. The tubes are incubated for 24 hours at 370 °C in a shaking incubator at 120-150 rpm. The tubes will be inspected for evident bacterial growth after 24 hours of incubation. The turbidity generated by the bacteria will be measured using a UV-Visible spectrometer by determining the optical density at 600 nm. The lower the turbidity, the lower the optical density, and the stronger the antibacterial activity of the nanoparticle. The lowest concentration of silver nanoparticles that inhibited growth (MIC) showed the least inhibitory concentration. The formula calculates the percentage of antimicrobial activity:

$$\% \text{ of antimicrobial activity} = \left(\frac{Absorbance\ of\ control - Absorbance\ of\ sample}{Absorbance\ of\ control}\right) \times 100$$

where, control is the liquid media with bacterial inoculum without the nanoparticle.

In the agar well diffusion method, sterilized agar medium is placed onto Petri plates and allowed to harden before streaking the bacterial inoculum uniformly with a spreader. The cavities on the agar plates, known as wells, are created with a cork borer. Various volumes/concentrations of nanoparticle solution are pipetted into this well and incubated for 24 hours at 37 °C. After 24 hours, the plates will be manually viewed, and the clearing zone will be measured using a millimeter scale. The inhibitory action of the nanoparticle solution increases as the clearing zone increases.

3.7. Antifungal activity.

The antifungal activity is evaluated using well diffusion or disc diffusion techniques, in which the nutritional medium is put into hardened plates, as depicted in Figure 3. The fungal spores are injected into the plates and evenly distributed, following which the wells for the well diffusion method are formed.

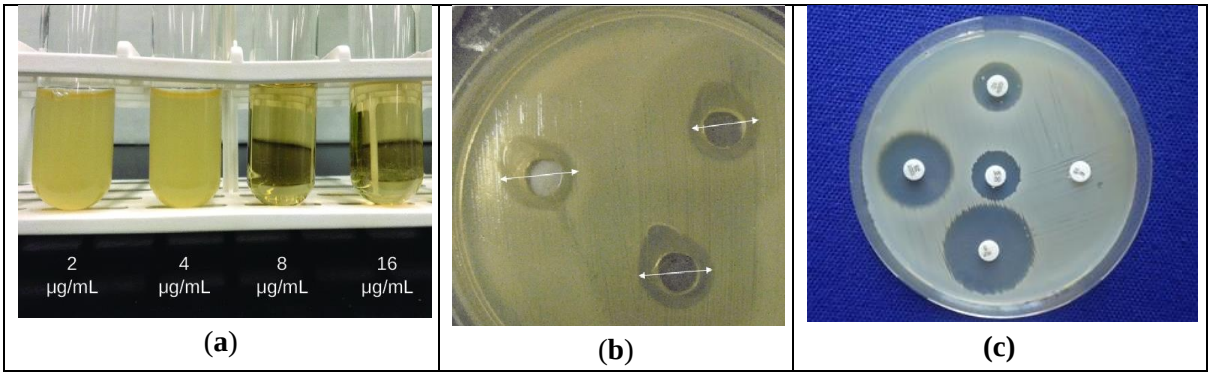

Figure 3. Pictorial representation of (**a**) broth dilution, (**b**)well diffusion, (**c**) disc diffusion involved in the evaluation of the antibacterial and antifungal activity of silver nanoparticles.

The nanoparticle solution is pipetted to test its antifungal activity. Alternatively, the nanoparticle solution is impregnated into sterile discs and placed on the plates to examine its antifungal activity. The plates are subsequently incubated at 25-27 °C for 3 to 4 days to detect the nanoparticle's suppression of mycelial growth. Less mycelial development or a larger clearing zone suggests that the nanoparticles have better antifungal effectiveness.

3.8. Photocatalytic.

The optimum quantity of AgNPs is dispersed in the dye medium. Photocatalytic dye degradation efficiency (D) can be estimated from the following equation:

$$D = \left(\frac{A_0 - A_t}{A_0}\right) \times 100\ \%$$

where, A_0 is the absorbance before dye degradation and A_t is the UV-Visible absorbance after dye degradation in the presence of AgNPs.

The first-order kinetic study on the dye degradation reaction of different dyes can be evaluated using the following equation:

$$\ln\left(\frac{A_0}{A_t}\right) = kt$$

where, k is the rate constant, A_0, and A_t is the initial and final UV-Visible absorbance before and after degradations of dye.

4. Applicative properties of Silver Nanoparticles

4.1. Antibacterial activity of silver nanoparticles by green synthesis.

The silver nanoparticles produced by the aqueous extracts of *Parkia biglandulosa* leaves showed a 12 mm inhibition zone against *Bacillus cereus* at a concentration of 0.02M. In contrast, higher concentrations reduced the antimicrobial activity [47]. The AgNPs synthesized from the fruit extracts of *Olea europaea* showed a 22 mm inhibition zone against *Streptococcus mutans* in the presence of 100µL/mL of silver nitrate solution. The antimicrobial activity increased as the concentration was increased [48]. The antibacterial effect of AgNPs obtained from different plant extracts (water, acetone, petroleum ether, and methanol) of certain weeds (*Lantana camara*, *Parthenium hysterophorus*, *Oxalis corniculata*, *Leucas aspera*, and *Tridax procumbens*) were examined. The highest antimicrobial activity against *Escherichia coli* was reported to be in aqueous extract of *Oxalis corniculata* (40 mm clearing zone), while against *Klebsiella pneumoniae* was seen in petroleum ether extract of *Oxalis corniculata* (20 mm) and against *Staphylococcus aureus* was observed in aqueous extract of *Leucas aspera* (24 mm) [49]**.** AgNPs synthesized from Aqueous extracts of *Nyctanthes arbor-tritis* showed bactericidal effects on *E. coli*, *S. aureus,* and *Shewanella putrefaciens.* As the concentrations of AgNPs increased from 0.006 – 0.2%, the antibacterial effect on all these three strains increased from 11.2 to 22.3mm zone of inhibition [50]. In AgNPs synthesized from *Marphysa moribidii* (Annelida) showed antimicrobial effects against both gram-positive as well as gram-negative bacteria. The highest activity was observed against *S. epidermidis* (9.18 mm), followed by

Pseudomonas aeruginosa (8.94 mm), and the least was observed against *K. pnuemoniae* (6.00 mm). However, the antimicrobial activity of these AgNPs was significantly lesser than those of commercially available antibiotics like gentamycin [51]. When AgNPs were formed using the extracts of *Lactobacillus reuteri*, they showed an 8 mm inhibition zone against *E.coli* and 10 mm against *Bacillus subtilis* when 20 µL of AgNp solution was used [52]. Using the exopolysaccharides produced from *B. subtilis* the AgNPs synthesized were impregnated into the linen fabrics to check the antimicrobial activity. It showed an average of 94% inhibition against *S. aureus* and 90% against *E. coli*. Also, it was noted after 20 cycles of laundering, the antimicrobial effect of the fabric were reduced to 75% against *S. aureus* and 70% against *E. coli* [53]. The biosynthesized AgNPs from the tubers of *Gloriosa superba* showed antibacterial effects against *Enterococcus faecalis* (29 mm), *B. subtilis* (24 mm), and *S. aureus* (23 mm) at 40 µg/mL concentration [54] The fruit peel extract of *Vitis vinifera* was used as a reductant to synthesize the AgNPs, and its antimicrobial activity was tested against potential pathogenic bacteria like *S. aureus, S. epidermidis* and *Listeria monocytogenes* at a concentration of 1mg/ml. There was a positive result as the fruit peel extract showed no inhibition zone while the doped AgNPs showed a zone of inhibition against all the bacteria used for the study [55]**.** Similarly, in another study, the essential oils of oregano, thyme, clove, and rosemary were used as a reductant for forming AgNPs, and their antimicrobial activity was checked against *E. coli*, *S. aureus,* and *B. cereus*. The AgNPs formed due to the clove oil was found to have a minimum inhibitory conc. at 40 µg/mL against *S. aureus* while they had no effect on other organisms [56] AgNPs synthesized from aqueous extracts of *Sapindus mukorossi* fruit pericarps showed similar antibacterial effects on both gram-negative and gram-positive bacterium. They also reported that higher concentrations showed larger clearing zones. 60 µg/mL showed 27.3 and 12.0 mm clearing zone against *S. aureus* and *P. aeruginosa*, respectively. The bactericidal effect of synthesized AgNPs was almost equivalent to the activity of standard antibiotic streptomycin against the *S. aureus* cultures [57]**.** Similarly, the AgNPs synthesized from *Zataria multiflora* also showed antibacterial effects on *S. aureus*. 4 µg/mL of green synthesized Nps showed minimum inhibitory activity, while the commercial Nps exhibited minimum inhibitory activity at 8 µg/mL. Also, it was noted that higher concentrations of Nps caused strong biofilm inhibitory activity [58]**.** The AgNPs synthesized from aqueous extracts of *Scutellaria barbata* showed antimicrobial activity against *E. coli* (21 mm), *S. aureus* (20 mm), *P. aeruginosa* (21 mm), and *K. pneumoniae* (22 mm) at 60 µg/mL [59]**.** *Aloe vera* gel was used as a reductant, and AgNPs were synthesized, which showed a strong antibacterial effect against *Enterobacter* sps. (32 mm) followed by *S. aureus* (21 mm), and the least was observed in *P. aeruginosa* (14 mm) [60]. The AgNPs synthesized with arabinoxylan extracted from *Andrographis paniculata* showed bactericidal activity against *S. pneumonia* (12.06 mm) and *E. coli* (12.03 mm) [61]**.** The AgNPs synthesized from *Coriander sativum* showed maximum inhibitory activity against *S. aureus* (13 mm) followed by *S. epidermidis* (12 mm), and the least was observed in *K. pneumoniae* and *P. aeruginosa* (9 mm) [62]**.** The AgNPs biosynthesized from *Citrus limetta* peel extracts showed maximum inhibitory activity against *E. coli* (12.5 mm) and *Streptococcus mutans* (12 mm), while the least activity was seen in *Micrococcus luteus* (11 mm) [63]. Click or tap here to enter text. The AgNPs synthesized from *Brillantaisia patula, Crossopteryx febrifuga,* and *Senna siamea* also showed an antibacterial effect on *E. coli, S. aureus,* and *P. aeruginosa* [64]. Seeds of *Moringa oleifera* mediated AgNPs showed a strong bactericidal effect against *E. coli* (30.6 mm), followed by *Salmonella enterica* (29 mm), *P. aeruginosa* (22.8 mm), and the least was observed in *S. aureus* (14.6 mm) [65].Click or tap

here to enter text. *Calendula officinalis* flower extracts were used to synthesize AgNPs, and their antimicrobial activity was checked against a plant pathogen, namely, *Pectobacterium caratovorum*. 40 ppm concentration showed a minimum inhibitory effect against the pathogen; however, the highest inhibitory effect was seen at 160 ppm. The AgNPs also prevented biofilm formation at 40 ppm [66].Click or tap here to enter text. The AgNPs synthesized from aqueous extracts of Tasmanian flax-lily leaves showed the highest inhibitory effect against *S. aureus* (94%), followed by *P. aeruginosa* (93.68%) and *S. epidermidis* (91.57%) [67] Click or tap here to enter text. The AgNPs synthesized from *Rivina humilis* showed antimicrobial activity against *Brucella* species. 800 µg/mL showed the highest inhibition zone against *B. abortus*, *B. melitensis,* and *B. suis,* equivalent to its standard antibiotic drug. While 1200 µg/mL showed the highest inhibition zone against B. cereus (12 mm), *S. aureus* (11 mm), *B. subtilis* (10 mm), *E. aerogenes* (12 mm), *Shigella flexineri* (13 mm), and *E. coli* (12.5 mm) [68].Click or tap here to enter text. AgNPs synthesized from aqueous extracts of *Symplocos racemosa* showed a maximum zone of inhibition (27 mm) at a concentration of 200 mg/mL and the least (20 mm) at a concentration of 50 mg/mL against *P. aeruginosa* [69].Click or tap here to enter text. The AgNPs synthesized from aqueous leaf extracts of *Gomphrena globosa* showed a maximum zone of inhibition against *S. aureus* (24 mm), followed by *E. coli* (22 mm), K. pneumonia (15 mm), *B. subtilis*, *M. luteus* and *P. aeruginosa* all showing 14 mm inhibition zone when 5 mL of Np was impregnated to the disc. As the volume increased, the antibacterial effect decreased [70]. The AgNPs synthesized from tea leaf extracts showed a clearing zone of 27 mm against *Streptomyces albidoflavus* at a conc. of 0.005% [71].

4.2. Antifungal activity of silver nanoparticles by green synthesis.

AgNPs synthesized from *Bacillus* sp. extract inhibited the hyphal growth of *Colletotrichum falcatum* and showed the highest antifungal activity at conc. ranging from 10-20 µg/mL [72]. The *Olea europaea* AgNp extracts also showed antifungal activity against *Candida albicans* whose inhibition zone was noted to be 13 mm for 100µL/mL concentration [48]**.** The AgNPs synthesized from arabinoxylan extracted from *Andrographis paniculata* also showed a similar result against *C. albicans* (10.77 mm) [61]**.** While the AgNPs synthesized from *Citrus limetta* peel extracts showed antifungal activity against various strains of Candia like *C. albicans* (15 mm), *C. glabrata, C. tropicalis,* and *C. parapsilosis,* all showed a 14 mm growth inhibition zone. The AgNPs synthesized from Tasmanian flax-lily showed an inhibitory percentage of 89.94 against *C. albicans* [67]. Leaf extract of *Malva parviflora* was used for the biosynthesis of AgNPs and further used for the study of antifungal activity against *Helminthosporium rostratum*, *Fusarium solani*, *Fusarium oxysporum*, and *Alternaria alternata.* The maximum mycelial growth inhibition was observed against *H. rostratum* (88.6%), followed by *A. alternata* (83.0%), *F. solani* (81.1%), and the least was observed in *F. oxysporum* (80.7%) [73]. The AgNPs synthesized from Tea tree leaf extracts were used to determine the antifungal activity in different concentrations (0.005, 0.01, 0.0125%). The inhibition zone with the lowest concentration was 11, 17, and 18 mm against *Aspergillus fumigatus*, *Byssochlamys spectabilis,* and *Cladosporium xanthochromaticum,* respectively [71].

4.3. General mechanism of antimicrobial activity of silver nanoparticles.

When mixed with other natural chemicals during the green manufacturing process, silver nanoparticles show a substantial boost in antibacterial activity owing to the breakdown of the microorganisms' cell membrane [74]. Because of their extremely small size, AgNPs readily penetrate the bacterial membrane and block cellular oxidation in the mitochondria, finally killing the bacterium [14], shown in Figure 4. According to McQuillan et al., the fundamental action of antibacterial activity is the total breakdown of the bacterial cell wall [75]. Because bacteria have a peptidoglycan cell wall, silver nanoparticles are poisonous to them but not to humans. As a result, the silver nanoparticles disintegrate the peptidoglycan cell wall. The antimicrobial sensitivity of certain bacteria varies to a larger extent depending on the makeup of their cell walls. The AgNPs are oxidized to silver ions in the cellular environment, adding to antibacterial action [74]. Silver ions have been shown to disrupt DNA replication and gene expression mechanisms [76]. The process comprises three key findings: cell membrane disruption, silver ion intake reduces potassium levels and impacts ATP synthesis, and the formation of Reactive Oxygen Species (ROS) and other free radicals [77]. The structure of the NP is also important for antibacterial action [78]. Pal *et al.* discovered that truncated triangular NP had greater antibacterial action against *E. coli* than spherical and rod-shaped particles [79]. The smaller the NP's size, the higher its antimicrobial activity efficiency. This is due to its greater penetration into bacterial cells [51, 55, 76]**.** Click or tap here to enter text.

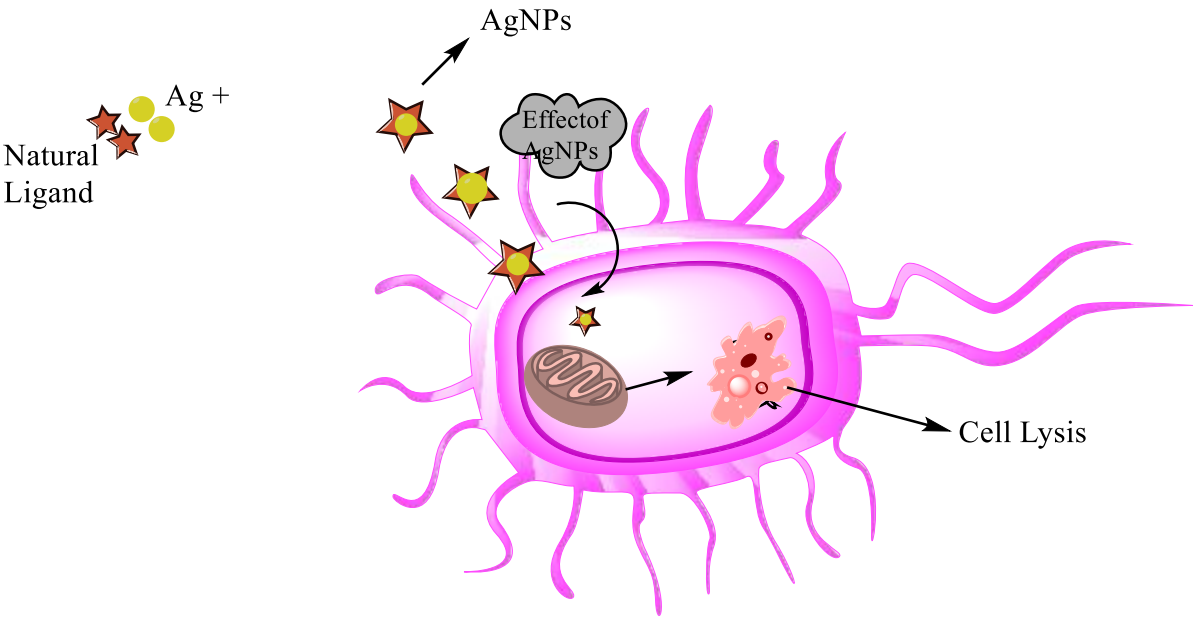

Figure 4. General mechanism of antimicrobial activity of silver nanoparticles.

4.4. Catalytic properties of Ag NPs.

With increasing population, commercialization, and civilizations, the usage of organic dyes in everyday life is expanding. Synthetic organic dyes are used in various sectors, including food, leather, pharmaceuticals, cosmetics, paints, plastics, paper, and textiles. The most difficult problem in the post-production of products from these sectors is the management of organic dyes, which migrate to water bodies via wastewater. These synthetic hues (organic dyes) harm human health and the environment. Traditional color removal procedures have included coagulation, filtration, adsorption, and reverse osmosis. Despite this, these hues are

difficult to remove from water because of their aromatic structural stability. Nano-catalysts are one of the most promising agents for reducing synthetic dyes.

To date, green synthesized AgNPs mediated photocatalytic degradation of methylene blue under sunlight has been reported. Exposure to sun radiation (exposure time) plays a key role in the photocatalytic degradation activity of AgNPs. In this process, the color change from dark blue to light blue/colorless after some reaction time will be examined. That is, the absorption intensity of the dye decreases with exposure time, which can be evaluated by measuring the absorbance using a UV-Visible spectrometer. Reduction in the absorption intensity signifies the reduction of the dye, indicating dye degradation in the presence of AgNPs. In addition, the degradation rate also depends on various parameters such as the size of the particles, structure, morphology, and concentration of the silver nanoparticles. Among these, the size of the particles (AgNPs) is an important parameter in dye degradation. e Smaller the particle's size, the larger the surface-to-volume ratio, and the higher the adsorption to the reactants (organic dye), thus increasing the rate of reaction (dye degradation). It is reported that the AgNPs are the mediators of transferring the electrons in the dye degradation process. It is also reported that photocatalytic activity may be due to the excitation of surface plasmon resonance (SPR) of AgNPs. That is, the dye degradation rate accelerated by the photonic excitation of AgNPs. The mechanism of dye degradation by AgNPs in the presence of sunlight is given in Figure 5.

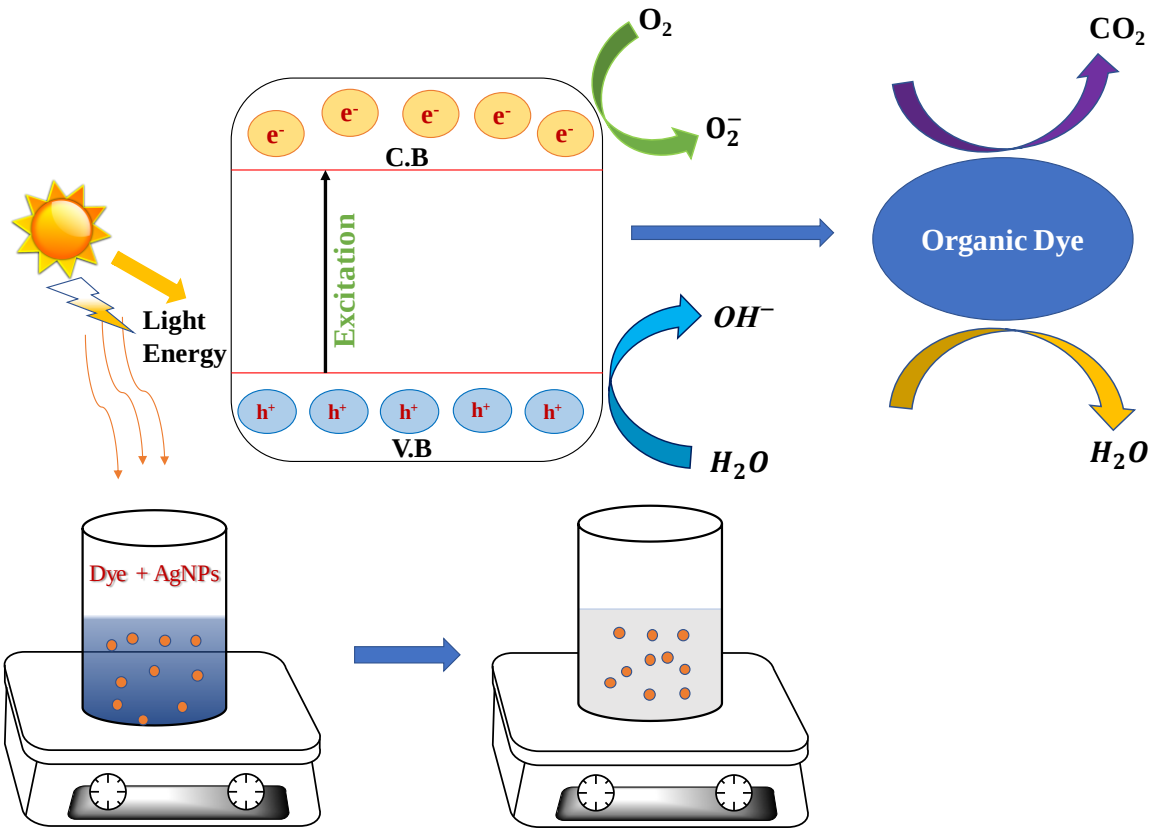

Figure 5. General method and mechanism of dye degradation by silver nanoparticles.

Numerous papers have been published on the photocatalytic activity of green-produced silver nanoparticles on various dyes, including Methylene Blue (MB) [80-83], Rhodamine B [82, 84-86], Nitrophenol [82, 87-88], Congo Red [89] Click or tap here to enter text., $KMnO_4$ [89], Hexavalent Chromium [90], Crystal Violet [88]Click or tap here to enter text., Coomassie Brilliant Blue [88], Textile Dye [91-92], methyl orange [88, 93], Orange G [93]. Furthermore, green-produced silver nanoparticles are employed to break down active pharmaceutical

ingredients (APIs) such as paracetamol [94]. Carcinogenic organic solvents such as benzene, toluene, and phenol are degraded [95]. Table 1 shows the results of competitive research on dye degradation for several dyes. J. Saha *et al.* [80] reported 100 % degradation of methylene blue in the presence of 3.0 mL of silver nanoparticles with an average size of 17 nm within 10 minutes. Furthermore, R. Banu *et al.* [82] found that the optimal amount of AgNP for MB degradation was around 100 L with an average size of 15 and the degradation of Rhodamine B and 4-Nitrophenol. Furthermore, F. Baghbani-Arani *et al.* [96] showed 100% effectiveness degradation of Coomassie Brilliant Blue G-250 under UV radiation after 60 minutes of exposure. It has been discovered that the size of silver nanoparticles has an important impact on the degradation of various colors. The smaller the silver particle, the faster it degrades and is more effective. Furthermore, the concentration of silver nanoparticles influences effectiveness and dye degradation; the higher the concentration, the greater the dye degradation.

Table 1. Summary on the comparison of various dye degradation with the presence of silver nanoparticles.

Ref.	Plant / Extract	Size of AgNPs / (nm)	Target Dye	Degradation
[80]	fruit extract of Gmelina Arborea	17	Methylene Blue (MB)	100% degradation within 30 min with 1.5 mL of AgNPs and within 10 min with 3.0 mL of AgNPs.
[81]	Honey	5 - 25	MB	92% degradation for 72 h.
[82]	Bael Gum (BG)	15	MB, Rhodamine B 4-Nitrophenol	The optimizing quantity of AgNP is 100 µL.
[83]	Catharanthus roseus	7	MB	98 % degradation with 100 mM AgNPs within 5 mins.
[85]	Kalanchoe pinnata	40	Rhodamine B (RhB) dye	83 % degradation in 45minutes under UV radiation.
[88]	Trigonella foenum-graecum seed	< 100	RhB	93 % degradation under UV.
[87]	Fucus gardeneri	20	Nitrophenol	96.4 % degradation within 5 min.
[88]	Ruellia tuberosa	56	Crystal violet, Coomassie brilliant blue	87 % degradation towards crystal violet and 74% degradation of coomassie brilliant blue within 30 minutes.
[89]	Neem leaves	3	Congo Red, KMnO4	100 % degradation of Congo Red within 15 mins and KMnO4 within 90 minutes.
[91]	Bacillus marisflavi	11 – 40	Textile dye	67 % degradation after 52 hours of exposure under sunlight with AgNPs concentration of 100 mg/L.
[92]	Nigella Sativa seed	10	Textile dye	98.5 % degradation of CR dye within 13 minutes.
[93]	Alpinia nigra	6	RhB, Methyl orange, Orange G	85.9 %, 83.4%, and 79.9% degradation of RhB, methyl orange, and orange G in the presence of sunlight.
[96]	Artemisia tournefortiana Rchb	23	Coomassie Brilliant Blue G-250	100 % efficacy within 60 min under UV light.
[97]	Chlorella vulgaris	55	MB	96.5 % degradation within 3 hours.

4. Conclusions

In this review study, we discussed the significance of green synthesis methods for producing silver nanoparticles utilizing various plant-mediated extracts and their antibacterial and photocatalytic characteristics. We also provided a general synthesis method and various spectroscopic characterizations, though the characterization techniques apply to all types of

nanoparticles to investigate the structural, microstructural, optical, and other physical properties of green synthesized silver nanoparticles. Nanosilver particles have been widely employed for various purposes in the modern era due to their toxicity. We also established a generic mechanism for antibacterial activity against various microorganisms and the photocatalytic activity of silver nanoparticles against various industrial dyes.

Funding

This research received no external funding.

Acknowledgments

This research has no acknowledgment.

Conflicts of Interest

The authors declare no conflict of interest.

References

1. Liu, W.T. Nanoparticles and their biological and environmental applications. *J. Biosci. Bioeng.* **2006**, *102*, 1–7, https://doi.org/10.1263/jbb.102.1.
2. Ealias, A.M.; Saravanakumar, M.P. A review on the classification, characterisation, synthesis of nanoparticles and their application. *IOP Conf. Series: Mater. Sci. Eng.* **2017**, *263*, 032019, http://dx.doi.org/10.1088/1757-899X/263/3/032019.
3. Hall, J.B.; Dobrovolskaia, M.A.; Patri, A.K.; McNeil, S.E. Characterization of nanoparticles for therapeutics. *Nanomed.* **2007**, *2*, 789–803, https://doi.org/10.2217/17435889.2.6.789.
4. Pal, S. The Ayurvedic Bhasma: The Ancient Science of Nanomedicine. *Rec. Pat. Nanomed.* **2015**, *5*, 12–18, http://dx.doi.org/10.2174/1877912305666150417233945.
5. Singh, R.K.; Kumar, S.; Aman, A.K.; Karim, S.M.; Kumar, S.; Kar, M. Study on physical properties of Ayurvedic nanocrystalline Tamra Bhasma by employing modern scientific tools. *J. Ayur. Integ. Med.* **2019**, *10*, 88–93, https://doi.org/10.1016/j.jaim.2017.06.012.
6. Sharma, R.; Prajapati, P.K. Nanotechnology in medicine: Leads from Ayurveda. *J. Pharm. Bioall. Sci.* **2016**, *8*, 80–81, https://doi.org/10.4103/0975-7406.171730.
7. Sarkar, P.K.; Chaudhary, A.K. Ayurvedic Bhasma: the most ancient application of nanomedicine. *J. Sci. Indus. Res.* **2010**, *69*, 901-905.
8. Hasan, S. A Review on Nanoparticles: Their Synthesis and Types. *Res. J. Recent. Sci.* **2015**, *4*, 1-3.
9. Lu, X.; Rycenga, M.; Skrabalak, S.E.; Wiley, B.; Xia, Y. Chemical synthesis of novel plasmonic nanoparticles. *Ann. Rev. Phy. Chem.* **2009**, *60*, 167–192, https://doi.org/10.1146/annurev.physchem.040808.090434.
10. Singh, P.; Kim, Y.J.; Zhang, D.; Yang, D.C. Biological Synthesis of Nanoparticles from Plants and Microorganisms. *Trend. Biotech.* **2016**, *34*, 588–599, https://doi.org/10.1016/j.tibtech.2016.02.006.
11. Gericke M.; Pinches, A. Biological synthesis of metal nanoparticles. *Hydromet.* **2006**, *83*, 132–140, https://doi.org/10.1016/j.hydromet.2006.03.019.
12. Midha, K.; Singh, G.; Nagpal, M.; Arora, S. Potential Application of Silver Nanoparticles in Medicine. *Nanosci. Nanotechn.-Asia* **2017**, *6*, 82–91, http://dx.doi.org/10.2174/2210681205666150818230319.
13. Singh, M.; Singh, S.; Prasad, S.; Gambhir, I.S. Nanotechnology in medicine and antibacterial effect of silver nanoparticles. *Dig. J. Nanomat. Biostruct.* **2008**, *3*, 115 – 122.
14. Wong, K.K.Y.; Liu, X. Silver nanoparticles - The real 'silver bullet' in clinical medicine? *Med. Chem. Comm.* **2010**, *1*, 125–131, http://dx.doi.org/10.1039/c0md00069h.
15. Baker, C.; Pradhan, A.; Pakstis, L.; Pochan, D.J.; Shah, S.I. Synthesis and antibacterial properties of silver nanoparticles. *J. Nanosci. Nanotechn.* **2005**, *5*, 244–249, http://dx.doi.org/10.1166/jnn.2005.034.
16. Vidhu, V.K.; Philip, D. Catalytic degradation of organic dyes using biosynthesized silver nanoparticles. *Micron* **2014**, *56*, 54–62, https://doi.org/10.1016/j.micron.2013.10.006.

17. Heilmann, A.; Keisow, A.; Gruner, M.; Kreibig, U. Optical and electrical properties of embedded silver nanoparticles at low temperatures. *Thin Solid Films* **1999**, *343-344*, 175-178, https://doi.org/10.1016/S0040-6090(98)01599-5.
18. Rafique, M.; Sadaf, I.; Rafique, M.S.; Tahir, M.B. A review on green synthesis of silver nanoparticles and their applications. *Art. Cell. Nanomed. Biotechn.* **2017**, *45*, 1272–1291, https://doi.org/10.1080/21691401.2016.1241792.
19. Ghaffari-Moghaddam, M.; Hadi-Dabanlou, R.; Khajeh, M.; Rakhshanipour, M.; Shameli, K. Green synthesis of silver nanoparticles using plant extracts. *Korean J. Chem. Eng.* **2014**, *31*, 548–557, http://dx.doi.org/10.1007/s11814-014-0014-6.
20. Iravani, S.; Korbekandi, H.; Mirmohammadi, S.V.; Zolfaghari, B. Synthesis of silver nanoparticles: chemical, physical and biological methods. *Res Pharm Sci.* **2014**, *9*, 385–406.
21. Harra, J.; Makitalo, J.; Siikanen, R.; Virkki, M.; Genty, G.; Kobayashi, T.; Kauranen, M.; Makela, J.M. Size-controlled aerosol synthesis of silver nanoparticles for plasmonic materials. *J. Nanopart. Res.* **2012**, *14*, 870–879, http://dx.doi.org/10.1007/s11051-012-0870-0.
22. Rafique, M.; Rafique, M.S.; Kalsoom, U.; Afzal, A.; Butt, S.H.; Usman, A. Laser ablation synthesis of silver nanoparticles in water and dependence on laser nature. *Opt. Quant. Elect.* **2019**, *51*, 179, https://link.springer.com/article/10.1007/s11082-019-1902-0.
23. Sudha, S.S.; Rajamanickam, K.; Rengaramanujam, J. Microalgae mediated synthesis of silver nanoparticles and their antibacterial activity against pathogenic bacteria. *Indian. J. Exp. Biol.* **2013**, *51*, 393-399.
24. Feroze, N.; Arshad, B.; Younas, M.; Afridi, M.I.; Saqib, S.; Ayaz, A. Fungal mediated synthesis of silver nanoparticles and evaluation of antibacterial activity. *Microscop. Res. Techn.* **2020**, *83*, 72–80, http://dx.doi.org/10.1002/jemt.23390.
25. Ahmed, S.; Ahmad, M.; Swami, B.L.; Ikram, S. A review on plants extract mediated synthesis of silver nanoparticles for antimicrobial applications: A green expertise. *J. Adv. Res.* **2016**, *7*, 17–28, https://doi.org/10.1016/j.jare.2015.02.007.
26. Logaranjan, K.; Raiza, A.J.; Gopinath, S.C.B.; Chen, Y.; Pandian, K. Shape- and Size-Controlled Synthesis of Silver Nanoparticles Using Aloe vera Plant Extract and Their Antimicrobial Activity. *Nanosca. Res. Lett.* **2016**, *11*, 520, https://doi.org/10.1186/s11671-016-1725-x.
27. Emeka, E.E.; Ojiefoh, O.C.; Aleruchi, C.; Hassan, L.A.; Christiana, O.M.; Rebecca, M.; Dare, E.O.; Temitope, A.E. Evaluation of antibacterial activities of silver nanoparticles green-synthesized using pineapple leaf (Ananas comosus). *Micron* **2014**, *57*, 1–5, https://doi.org/10.1016/j.micron.2013.09.003.
28. Mariselvam, R.; Ranjitsingh, A.J.A.; Nanthini, A.U.R.; Kalirajan, K.; Padmalatha, C.; Selvakumar, P.M. Green synthesis of silver nanoparticles from the extract of the inflorescence of Cocos nucifera (Family: Arecaceae) for enhanced antibacterial activity. *Spectrochim. Act. - Part A: Mol. Biomol. Spec.* **2014**, *129*, 537–541, https://doi.org/10.1016/j.saa.2014.03.066.
29. Saxena, A.; Tripathi, R.M.; Zafar, F.; Singh, P. Green synthesis of silver nanoparticles using aqueous solution of Ficus benghalensis leaf extract and characterization of their antibacterial activity. *Mat. Lett.* **2012**, *67*, 91–94, https://doi.org/10.1016/j.matlet.2011.09.038.
30. Verma, A.; Mehata, M.S. Controllable synthesis of silver nanoparticles using Neem leaves and their antimicrobial activity. *J. Rad. Res. Appl. Sci.* **2016**, *9*, 109–115, https://doi.org/10.1016/j.jrras.2015.11.001.
31. Basu, S.; Maji, P.; Ganguly, J. Rapid green synthesis of silver nanoparticles by aqueous extract of seeds of *Nyctanthes arbor-tristis*. *Appl. Nanosci.* **2016**, *6*, 1-5, http://dx.doi.org/10.1007/s13204-015-0407-9.
32. Sharma, S.; Kumar, A.; Kaur, K. Synthesis, characterization and antibacterial potential of silver nanoparticles by Morus nigra leaf extract. *Indian J. Pharm. Bio. Res.* **2013**, *1*, 16-24, http://dx.doi.org/10.30750/ijpbr.1.4.4.
33. Sable, N.; Gaikwad, S.; Bonde, S.; Gade, A.; Rai, M. Phytofabrication of silver nanoparticles by using aquatic plant Hydrilla verticillata. *Nusantara Biosci.* **2012**, *4*, 45-49, http://dx.doi.org/10.13057/nusbiosci/n040201.
34. Joseph, J.; Deborah, S.K.; Raghavi, R.; Shamya, A.M.; Aruni, W. Green synthesis of silver nanoparticles using *Phyllanthus amarus* Seeds and their antibacterial activity assessment. *Biomed. Biotechn. Res. J.* **2021**, *5*, 35–38.
35. Manikandan, R.; Manikandan, B.; Raman, T.; Arunagirinathan, K.; Prabhu, N.M.; Basu, M.J.; Perumal, M.; Palanisamy, S.; Munusamy, A. Biosynthesis of silver nanoparticles using ethanolic petals extract of Rosa indica and characterization of its antibacterial, anticancer and anti-inflammatory activities. *Spectrochim. Act. - Part A: Mol. Biomol. Spec.* **2015**, 138, 120–129, https://doi.org/10.1016/j.saa.2014.10.043.
36. Joseph, S.; Mathew, B. Facile synthesis of silver nanoparticles and their application in dye degradation. *Mat. Sci. Eng. B* **2015**, *195*, 90–97, https://doi.org/10.1016/j.mseb.2015.02.007.

37. Zamarchi, F.; Vieira, I.C. Determination of paracetamol using a sensor based on green synthesis of silver nanoparticles in plant extract. *J. Pharm. Biomed. Anal.* **2021**, *196*, 113912, https://doi.org/10.1016/j.jpba.2021.113912.
38. Sheng, Z.; Liu, Y. Effects of silver nanoparticles on wastewater biofilms. *Water Res.* **2011**, *45*, 6039–6050, https://doi.org/10.1016/j.watres.2011.08.065.
39. Hou, L.; Li, K.; Ding, Y.; Li, Y.; Chen, J.; Wu, X.; Li, X. Removal of silver nanoparticles in simulated wastewater treatment processes and its impact on COD and NH_4 reduction. *Chemosph.* **2012**, *87*, 248–252, https://doi.org/10.1016/j.chemosphere.2011.12.042.
40. Galdopórpora, J.M.; Ibar, A.; Tuttolomondo, M.V.; Desimone, M.F. Dual-effect core–shell polyphenol coated silver nanoparticles for tissue engineering. *Nano-Struct. Nano-Obj.* **2021**, *26*, 100716, https://doi.org/10.1016/j.nanoso.2021.100716.
41. Kokura, S.; Handa, O.; Takagi, T.; Ishikawa, T.; Naito, Y.; Yoshikawa, T. Silver nanoparticles as a safe preservative for use in cosmetics. *Nanomed.: Nanotechn. Bio. Med.* **2010**, *6*, 570–574, https://doi.org/10.1016/j.nano.2009.12.002.
42. Gajbhiye, S.; Sakharwade, S. Silver Nanoparticles in Cosmetics. *J. Cosm. Derm. Sci. Appl.* **2016**, *6*, 48–53, http://dx.doi.org/10.4236/jcdsa.2016.61007.
43. Knetsch, M.L.W.; Koole, L.H. New strategies in the development of antimicrobial coatings: The example of increasing usage of silver and silver nanoparticles. *Polym.* **2011**, *3*, 340–366, https://doi.org/10.3390/polym3010340.
44. Pollini, M.; Paladini, F.; Catalano, M.; Taurino, A.; Licciulli, A.; Maffezzoli, A.; Sannino, A. Antibacterial coatings on haemodialysis catheters by photochemical deposition of silver nanoparticles. *J. Mat. Sci.: Mat. Med.* **2011**, *22*, 2005–2012, https://doi.org/10.1007/s10856-011-4380-x.
45. Prasher, P.; Sharma, M.; Mudila, H.; Gupta, G.; Sharma, A.K.; Kumar, D.; Bakshi, H.A.; Negi, P.; Kapoor, D.N.; Chellappan, D.K.; Tambuwala, M.M.; Dua, K. Emerging trends in clinical implications of bio-conjugated silver nanoparticles in drug delivery. *Coll. Interf. Sci. Commun.* **2020**, *35*, 100244, https://doi.org/10.1016/j.colcom.2020.100244.
46. Adur, A.J.; Nandini, N.; Mayachar, K.S.; Ramya, R.; Srinatha, N. Bio-synthesis and antimicrobial activity of silver nanoparticles using anaerobically digested parthenium slurry. *J. Photochem. Photobio. B: Bio.* **2018**, *183*, 30-34, https://doi.org/10.1016/j.jphotobiol.2018.04.020.
47. John, A.; Shaji, A.; Velayudhannair, K.; Nidhin, M.; Krishnamoorthy, G. Anti-bacterial and biocompatibility properties of green synthesized silver nanoparticles using *Parkia biglandulosa* (Fabales:Fabaceae) leaf extract. *Curr. Res. Gr. Sust. Chem.* **2021**, *4*, 100112, https://doi.org/10.1016/j.crgsc.2021.100112.
48. Umai, D.; Vikranth, A; Meenambiga, S.S. A study on the green synthesis of silver nanoparticles from Olea europaea and its activity against oral pathogens. *Mat. Today: Proc.* **2021**, *44*, 3647–3651, https://doi.org/10.1016/j.matpr.2020.10.681.
49. Rakesh, B.; Chakraborty, I.; Sreelakshmi, L.V.; Preethi, S. Screening Of Anti-Microbial Activity Of Some Common Weeds By In-Vitro Green Synthesis Of Silver Nano Particles. *Int. J. Bio. Res.* **2020**, *8*, 14–24.
50. Sharma, L.; Dhiman, M.; Singh, A.; Sharma, M.M. Biological synthesis of silver nanoparticles using *Nyctanthes arbor-tristis* L.: A green approach to evaluate antimicrobial activities. *Mat. Today: Proc.* **2021**, *43*, 2915–2920, https://doi.org/10.1016/j.matpr.2021.01.208.
51. Rosman, N.S.R.; Harun, N.A.; Idris, I.; Ismail, W.I.W. Eco-friendly silver nanoparticles (AgNPs) fabricated by green synthesis using the crude extract of marine polychaete, *Marphysa moribidii*: biosynthesis, characterisation, and antibacterial applications. *Heliyon* **2020**, *6*, e05462, https://doi.org/10.1016/j.heliyon.2020.e05462.
52. Tharani, S.; Bharathi, D.; Ranjithkumar, R. Extracellular green synthesis of chitosan-silver nanoparticles using Lactobacillus reuteri for antibacterial applications. *Biocat. Agri. Biotech.* **2020**, *30*, 101838, https://doi.org/10.1016/j.bcab.2020.101838.
53. Abdelghaffar, F.; Mahmoud, M.G.; Asker, M.S.; Mohamed, S.S. Facile green silver nanoparticles synthesis to promote the antibacterial activity of cellulosic fabric. *J. Indus. Eng. Chem.* **2021**, *99*, 224–234, http://doi.org/10.1016/j.jiec.2021.04.030.
54. Murugesan, A.K.; Pannerselvam, B.; Javee, A.; Rajenderan, M.; Thiyagarajan, D. Facile green synthesis and characterization of Gloriosa superba L. tuber extract-capped silver nanoparticles (GST-AgNPs) and its potential antibacterial and anticancer activities against A549 human cancer cells. *Environ. Nanotechn. Monit. Manag.* **2021**, *15*, 100460, https://doi.org/10.1016/j.enmm.2021.100460.

55. Hashim, N.; Paramasivan, M.; Tan, J.S.; Kernain, D.; Hussain, M.H.; Brosse, N.; Gambier, F.; Raja, P.B. Green mode synthesis of silver nanoparticles using *Vitis vinifera's* tannin and screening its antimicrobial activity / apoptotic potential versus cancer cells. *Mat. Today Commun.* **2020**, *25*, 101511, https://doi.org/10.1016/j.mtcomm.2020.101511.
56. Vinicius de Oliveira Brisola Maciel, M.; Aline da Rosa, A.; Machado, M.H.; Elias, W.C.; Goncalves da Rosa, C.; Teixeira, G.L.; Noronha, C.M.; Bertoldi, F.C.; Nunes, M.R.; Dutra de Armas, R.; Barreto, P.L.M. Green synthesis, characteristics and antimicrobial activity of silver nanoparticles mediated by essential oils as reducing agents. *Biocat. Agri. Biotech.* **2020**, *28*, 101746, https://doi.org/10.1016/j.bcab.2020.101746.
57. Huong, V.T.L.; Nguyen, N.T. Green synthesis, characterization and antibacterial activity of silver nanoparticles using *Sapindus mukorossi* fruit pericarp extract. *Mat. Today: Proc.* **2019**, *42*, 88–93.
58. Barabadi, H.; Mojab, F.; Vahidi, H.; Marashi, B.; Talank, N.; Hosseini, O.; Saravanan, M. Green synthesis, characterization, antibacterial and biofilm inhibitory activity of silver nanoparticles compared to commercial silver nanoparticles. *Inorg. Chem. Commun.* **2021**, *129*, 108647, https://doi.org/10.1016/j.inoche.2021.108647.
59. Veeraraghavan, V.P.; Periadurai, N.D.; Karunakaran, T.; Hussain, S.; Surapaneni, K.M.; Jiao, X. Green synthesis of silver nanoparticles from aqueous extract of Scutellaria barbata and coating on the cotton fabric for antimicrobial applications and wound healing activity in fibroblast cells (L929). *Saudi J. Bio. Sci.* **2021**, *28*, 3633–3640, https://doi.org/10.1016/j.sjbs.2021.05.007.
60. Anju, T.R.; Parvathy, S.; Veettil, M.V.; Rosemary, J.; Ansalna, T.H.; Shaszabanu, M.M.; Devika, S. Green synthesis of silver nanoparticles from Aloe vera leaf extract and its antimicrobial activity. *Mat. Today: Proc.* **2020**, *43*, 3956–3960, http://dx.doi.org/10.1016/j.matpr.2021.02.665.
61. Maity, G.N.; Maity, P.; Choudhuri, I.; Sahoo, G.C.; Maity, N.; Ghosh, K.; Ghosh, K.; Bhattacharyya, N.; Dalai, S.; Mondal, S. Green synthesis, characterization, antimicrobial and cytotoxic effect of silver nanoparticles using arabinoxylan isolated from Kalmegh. *Int. J. Bio. Macromol.* **2020**, *162*, 1025–1034, https://doi.org/10.1016/j.ijbiomac.2020.06.215.
62. Alsubki, R.; Tabassum, H.; Abudawood, M.; Rabaan, A.A.; Alsobaie, S.F.; Ansar, S. Green synthesis, characterization, enhanced functionality and biological evaluation of silver nanoparticles based on Coriander sativum. *Saudi J. Bio. Sci.* **2021**, *28*, 2102–2108, https://doi.org/10.1016/j.sjbs.2020.12.055.
63. Dutta, T.; Ghosh, N.N.; Das, M.; Adhikary, R.; Mandal, V.; Chattopadhyay, A.P. Green synthesis of antibacterial and antifungal silver nanoparticles using *Citrus limetta* peel extract: Experimental and theoretical studies. *J. Env. Chem. Eng.* **2020**, *8*, 104019, https://doi.org/10.1016/j.jece.2020.104019.
64. Kambale, E.K.; Nkanga, C.I.; Mutonkole, B.P.I.; Bapolisi, A.M.; Tassa, D.O.; Liesse, J.-M.I.; Krause, R.W. M.; Memvanga, P.B. Green synthesis of antimicrobial silver nanoparticles using aqueous leaf extracts from three Congolese plant species (*Brillantaisia patula, Crossopteryx febrifuga* and *Senna siamea*). *Heliyon* **2020**, *6*, e04493, https://doi.org/10.1016/j.heliyon.2020.e04493.
65. Mehwish, H.M.; Rajoka, M.S.R.R.; Xiong, Y.; Cai, H.; Aadil, R.M.; Mahmood, Q.; He, Z.; Zhu, Q. Green synthesis of a silver nanoparticle using *Moringa oleifera* seed and its applications for antimicrobial and sunlight mediated photocatalytic water detoxification. *J. Env. Chem. Eng.* **2021**, *9*, 105290, https://doi.org/10.1016/j.jece.2021.105290.
66. Olfati, A.; Kahrizi, D.; Balaky, S.T.J.; Sharifi, R.; Tahir, M.B.; Darvishi, E. Green synthesis of nanoparticles using *Calendula officinalis* extract from silver sulfate and their antibacterial effects on *Pectobacterium caratovorum. Inorg. Chem. Commun.* **2020**, *125*, 108439, https://doi.org/10.1016/j.inoche.2020.108439.
67. Ahmed, S.R.; Anwar, H.; Ahmed, S.W.; Shah, M.R.; Ahmed, A.; Ali, S.A. Green synthesis of silver nanoparticles: Antimicrobial potential and chemosensing of a mutagenic drug nitrofurazone in real samples. *Measurement* **2021**, *180*, 109489, https://doi.org/10.1016/j.measurement.2021.109489.
68. Raghava, S.; Mbae, K.M.; Umesha, S. Green synthesis of silver nanoparticles by Rivina humilis leaf extract to tackle growth of Brucella species and other perilous pathogens. *Saudi J. Bio. Sci.* **2021**, *28*, 495–503, https://doi.org/10.1016/j.sjbs.2020.10.034.
69. Panda, M.K.; Dhal, N.K.; Kumar, M.; Mishra, P.M.; Behera, R.K. Green synthesis of silver nanoparticles and its potential effect on phytopathogens. *Mat. Today: Proc.* **2021**, *35*, 233–238, https://doi.org/10.1016/j.matpr.2020.05.188.
70. Tamilarasi, P.; Meena, P. Green synthesis of silver nanoparticles (Ag NPs) using Gomphrena globosa (Globe amaranth) leaf extract and their characterization. *Mat. Today: Proc.* **2019**, *33*, 2209–2216, https://doi.org/10.1016/j.matpr.2020.04.025.

71. Saada, N.S.; Abdel-Maksoud, G.; Abd El-Aziz, M.S.; Youssef, A.M. Green synthesis of silver nanoparticles, characterization, and use for sustainable preservation of historical parchment against microbial biodegradation. *Biocat. Agri. Biotech.* **2021**, *32*, 101948, https://doi.org/10.1016/j.bcab.2021.101948.
72. Ajaz, S.; Ahmed, T.; Shahid, M.; Noman, M.; Shah, A.A.; Mehmood, M.A.; Abbas, A.; Cheema, A.I.; Iqbal, M.Z.; Li, B. Bioinspired green synthesis of silver nanoparticles by using a native Bacillus sp. strain AW1-2: Characterization and antifungal activity against Colletotrichum falcatum Went. *Enzy. Microb. Techn.* **2020**, *144*, 109745, https://doi.org/10.1016/j.enzmictec.2021.109745.
73. Al-Otibi, F.; Perveen, K.; Al-Saif, N.A.; Alharbi, R.I.; Bokhari, N.A.; Albasher, G.; Al-Otaibi, R.M.; Al-Mosa, M.A. Biosynthesis of silver nanoparticles using Malva parviflora and their antifungal activity. *Saudi J. Bio. Sci.* **2021**, *28*, 2229–2235, https://doi.org/10.1016/j.sjbs.2021.01.012.
74. Durán, N.; Durán, M.; de Jesus, M.B.; Seabra, A.B.; Fávaro, W.J.; Nakazato, G. Silver nanoparticles: A new view on mechanistic aspects on antimicrobial activity. *Nanomed.: Nanotechn. Bio. Med.* **2016**, *12*, 789–799, https://doi.org/10.1016/j.nano.2015.11.016.
75. McQuillan, J.S.; Infante, H.G.; Stokes, E.; Shaw, A.M. Silver nanoparticle enhanced silver ion stress response in *Escherichia coli* K12. *Nanotox.* **2012**, *6*, 857–866, https://doi.org/10.3109/17435390.2011.626532.
76. Durán, N.; Marcato, P.D.; De Conti, R.; Alves, O.L.; Costa, F.T.M.; Brocchi, M. Potential use of silver nanoparticles on pathogenic bacteria, their toxicity and possible mechanisms of action. *J. Braz. Chem. Soc.* **2010**, *21*, 949–959, http://dx.doi.org/10.1590/S0103-50532010000600002.
77. Marambio-Jones, C.; Hoek, E.M.V. A review of the antibacterial effects of silver nanomaterials and potential implications for human health and the environment. *J. Nanopart. Res.* **2010**, *12*, 1531–1551, https://doi.org/10.1007/s11051-010-9900-y.
78. Sharma, V.K.; Yngard, R.A.; Lin, Y. Silver nanoparticles: Green synthesis and their antimicrobial activities. *Adv. Coll. Interf. Sci.* **2009**, *145*, 83–96, https://doi.org/10.1016/j.cis.2008.09.002.
79. Pal, S.; Tak, Y.K.; Song, J.M. Does the antibacterial activity of silver nanoparticles depend on the shape of the nanoparticle? A study of the gram-negative bacterium Escherichia coli. *Appl. Env. Microbiol.* **2007**, *73*, 1712–1720, https://doi.org/10.1128/aem.02218-06.
80. Saha, J.; Begum, A.; Mukherjee, A.; Kumar, S. A novel green synthesis of silver nanoparticles and their catalytic action in reduction of Methylene Blue dye. *Sust. Env. Res.* **2017**, *27*, 245–250 https://doi.org/10.1016/j.serj.2017.04.003.
81. Al-Zaban, M.I.; Mahmoud, M.A.; AlHarbi, M.A. Catalytic degradation of methylene blue using silver nanoparticles synthesized by honey. *Saudi J. Bio. Sci.* **2021**, *28*, 2007–2013, https://doi.org/10.1016/j.sjbs.2021.01.003.
82. Banu, R.; Ramakrishna, D.; Reddy, G.B.; Veerabhadram, G.; Mangatayaru, K.G. Facile one-pot microwave-assisted green synthesis of silver nanoparticles using Bael gum: Potential application as catalyst in the reduction of organic dyes. *Mat. Today: Proc.* **2021**, *43*, 2265–2273, http://dx.doi.org/10.1016/j.matpr.2020.12.861.
83. Rohaizad, A.; Shahabuddin, S.; Shahid, M.M.; Rashid, N.M.; Hir, Z.A.M.; Ramly, M.M.; Awang, K.; Siong, C.W.; Aspanut, Z. Green synthesis of silver nanoparticles from Catharanthus roseus dried bark extract deposited on graphene oxide for effective adsorption of methylene blue dye. *J. Env. Chem. Eng.* **2020**, *8*, 103955, https://doi.org/10.1016/j.jece.2020.103955.
84. Wang, Z.; Ye, X.; Chen, L.; Huang, P.; Wang, Q.; Ma, L.; Hua, N.; Liu, X.; Xiao, X.; Chen, S. Silver nanoparticles decorated grassy ZnO coating for photocatalytic activity enhancement. *Mat. Sci. Semicond. Proc.* **2021**, *121*, 105354, https://doi.org/10.1016/j.mssp.2020.105354.
85. Aryan; Ruby; Mehata, M.S. Green synthesis of silver nanoparticles using *Kalanchoe pinnata* leaves (life plant) and their antibacterial and photocatalytic activities. *Chem. Phys. Lett.* **2021**, *778*, 138760, https://doi.org/10.1016/j.cplett.2021.138760.
86. Awad, M.A.; Hendi, A.A.; Ortashi, K.M.; Alzahrani, B.; Soliman, D.; Alanazi, A.; Alenazi, W.; Taha, R.M.; Ramadan, R.; El-Tohamy, M.; AlMashoud, N.; Alomar, T.S. Biogenic synthesis of silver nanoparticles using Trigonella foenum-graecum seed extract: Characterization, photocatalytic and antibacterial activities. *Sens. Actu. A: Phys.* **2021**, *323*, 112670, https://doi.org/10.1016/j.sna.2021.112670.
87. Princy, K.F.; Gopinath, A. Green synthesis of silver nanoparticles using polar seaweed Fucus gardeneri and its catalytic efficacy in the reduction of nitrophenol. *Polar Sci.* **2021**, *30*, 100692, https://doi.org/10.1016/j.polar.2021.100692.
88. Seerangaraj, V.; Sathiyavimal, S.; Shankar, S.N.; Nandagopal, J.G.T.; Balashanmugam, P.; Al-Misned, F. A.; Shanmugavel, M.; Senthilkumar, P.; Pugazhendhi, A. Cytotoxic effects of silver nanoparticles on *Ruellia*

tuberosa: Photocatalytic degradation properties against crystal violet and coomassie brilliant blue. *J. Env. Chem. Eng.* **2021**, *9*, 105088, https://doi.org/10.1016/j.jece.2021.105088.
89. Zanjage, A.; Ali Khan, S. Ultra-fast synthesis of antibacterial and photo catalyst silver nanoparticles using neem leaves. *JCIS Open* **2021**, *3*, 100015, https://doi.org/10.1016/j.jciso.2021.100015.
90. Lakra, R.; Kiran, M.S.; Korrapati, P.S. Furfural mediated synthesis of silver nanoparticles for photocatalytic reduction of hexavalent chromium. *Env. Techn. Innov.* **2021**, *21*, 101348, https://doi.org/10.1016/j.eti.2020.101348.
91. Ahmed, T.; Noman, M.; Shahid, M.; Niazi, M.B.K.; Hussain, S.; Manzoor, N.; Wang, X.; Li, B. Green synthesis of silver nanoparticles transformed synthetic textile dye into less toxic intermediate molecules through LC-MS analysis and treated the actual wastewater. *Env. Res.* **2020**, *191*, 110142, https://doi.org/10.1016/j.envres.2020.110142.
92. Chand, K.; Jiao, C.; Lakhan, M.N.; Shah, A.H.; Kumar, V.; Fouad, D.E.; Chandio, M.B.; Maitlo, A.A.; Ahemed, M.; Cao, D. Green synthesis, characterization and photocatalytic activity of silver nanoparticles synthesized with Nigella Sativa seed extract. *Chem. Phys. Lett.* **2021**, *763*, 138218, https://doi.org/10.1016/j.cplett.2020.138218.
93. Baruah, D.; Yadav, R.N.S.; Yadav, A.; Das, A.M. *Alpinia nigra* fruits mediated synthesis of silver nanoparticles and their antimicrobial and photocatalytic activities. *J. Photochem. Photobio. B: Bio.* **2019**, *201*, 111649, https://doi.org/10.1016/j.jphotobiol.2019.111649.
94. Al-Gharibi, M.A.; Kyaw, H.H.; Al-Sabahi, J.N.; Myint, M.T.Z.; Al-Sharji, Z.A.; Al-Abri, M.Z. Silver nanoparticles decorated zinc oxide nanorods supported catalyst for photocatalytic degradation of paracetamol. *Mat. Sci. Semicond. Proc.* **2021**, *134*, 105994, https://doi.org/10.1016/j.mssp.2021.105994.
95. Ojha, A.; Singh, P.; Oraon, R.; Tiwary, D.; Mishra, A.K.; Ghfar, A.A.; Naushad, M.; Ahamad, T.; Thokchom, B.; Vijayaraghavan, K.; Rangabhashiyam, S. An environmental approach for the photodegradation of toxic pollutants from wastewater using silver nanoparticles decorated titania-reduced graphene oxide. *J. Env. Chem. Eng.* **2021**, *9*, 105622, https://doi.org/10.1016/j.jece.2021.105622.
96. Baghbani-Arani, F.; Movagharnia, R.; Sharifian, A.; Salehi, S.; Shandiz, S.A.S. Photo-catalytic, antibacterial, and anti-cancer properties of phyto-mediated synthesis of silver nanoparticles from Artemisia tournefortiana Rchb extract. *J. Photochem. Photobio. B: Bio.* **2017**, *173*, 640–649, https://doi.org/10.1016/j.jphotobiol.2017.07.003.
97. Rajkumar, R.; Ezhumalai, G.; Gnanadesigan, M. A green approach for the synthesis of silver nanoparticles by *Chlorella vulgaris* and its application in photocatalytic dye degradation activity. *Env. Techn. Innov.* **2021**, *21*, 101282, https://doi.org/10.1016/j.eti.2020.101282.